Eur Spine J (2014) 23:1384–1393
DOI 10.1007/s00586-013-3132-7

ORIGINAL ARTICLE

Pelvic incidence–lumbar lordosis mismatch results in increased segmental joint loads in the unfused and fused lumbar spine

Marco Senteler · Bernhard Weisse · Jess G. Snedeker · Dominique A. Rothenfluh

Received: 21 May 2013 / Revised: 8 December 2013 / Accepted: 8 December 2013 / Published online: 20 March 2014

Abstract

Purpose Symptomatic adjacent segment disease (ASD) has been reported to occur in up to 27 % of lumbar fusion patients. A previous study identified patients at risk according to the difference of pelvic incidence and lordosis. Patients with a difference between pelvic incidence and lumbar lordosis >15° have been found to have a 20 times higher risk for ASD. Therefore, it was the aim of the present study to investigate forces acting on the adjacent segment in relation to pelvic incidence–lumbar lordosis (PILL) mismatch as a measure of spino-pelvic alignment using rigid body modeling to decipher the underlying forces as potential contributors to degeneration of the adjacent segment.

Methods Sagittal configurations of 81 subjects were reconstructed in a musculoskeletal simulation environment. Lumbar spine height was normalized, and body and segmental mass properties were kept constant throughout the population to isolate the effect of sagittal alignment. A uniform forward/backward flexion movement (0°–30°–0°) was simulated for all subjects. Intervertebral joint loads at lumbar level L3–L4 and L4–L5 were determined before and after simulated fusion.

Results In the unfused state, an approximately linear relationship between sagittal alignment and intervertebral loads could be established (shear: 0° flexion $r = 0.36$, $p < 0.001$, 30° flexion $r = 0.48$, $p < 0.001$; compression: 0° flexion $r = 0.29$, $p < 0.01$, 30° flexion $r = 0.40$, $p < 0.001$). Additionally, shear changes during the transition from upright to 30° flexed posture were on average 32 % higher at level L3–L4 and 14 % higher at level L4–L5 in alignments that were clinically observed to be prone to ASD. Simulated fusion affected shear forces at the level L3–L4 by 15 % (L4–L5 fusion) and 23 % (L4–S1 fusion) more for alignments at risk for ASD.

Conclusion Higher adjacent segment shear forces in alignments at risk for ASD already prior to fusion provide a mechanistic explanation for the clinically observed correlation between PILL mismatch and rate of adjacent segment degeneration.

Keywords Musculoskeletal modeling · Spino-pelvic alignment · Lumbar fusion · Shear · Intervertebral disc degeneration · Adjacent segment degeneration

Introduction

Symptomatic adjacent segment disease (ASD) is observed in up to 27 % of patients and, therefore, presents a relevant clinical problem after lumbar spinal fusion surgery [1]. Mechanical loading, stiffness characteristics and intervertebral joint kinematics have been widely discussed as factors contributing to disc degeneration [2–5] and may

M. Senteler · J. G. Snedeker · D. A. Rothenfluh
Department of Orthopedics Balgrist, University of Zurich, Zurich, Switzerland

M. Senteler · J. G. Snedeker
Institute for Biomechanics, ETH Zürich, Zurich, Switzerland

M. Senteler · B. Weisse
Laboratory for Mechanical Systems Engineering, EMPA, Swiss Federal Laboratories for Materials Science and Technology, Dübendorf, Switzerland

D. A. Rothenfluh (✉)
Nuffield Orthopaedic Centre, Oxford University Hospitals NHS Trust, Oxford OX3 7HE, UK
e-mail: dominique.rothenfluh@mac.com

particularly contribute to the development of ASD. Considering static postures, forces acting on the intervertebral joints are predominantly a result of anatomy, body size, mass and muscular condition, all of which are reasonably distinctive among individuals.

In our preceding study, a relationship between pelvic incidence–lumbar lordosis (PILL) mismatch as a measure for spino-pelvic alignment and the risk for ASD was established based on a retrospective case–control study comparing patient groups matched for level and number of segments fused as well as preoperative degenerative changes in MR images. Using logistic regression and ROC analysis, a difference of pelvic incidence (PI) and lumbar lordosis (LL) of more than 15° was found to predict revision surgery for adjacent segment disease after lumbar spinal fusion with relatively high sensitivity and specificity. Patients were, therefore, grouped depending on whether the difference between PI and LL (ΔPILL = PI-LL) was $<15°$ (type A alignment) or $\geq 15°$ (type B alignment). The rate of revision surgery was 24.4 % in type A alignment and 87.2 % in type B alignment (accompanying ESJ manuscript, in revision).

The importance of spino-pelvic balance and its implications on the clinical treatment of low back pain patients was shown in recent studies [6, 7]. However, still little is known about how spino-pelvic alignment affects segmental joint forces, or how this may contribute to lumbar disc degeneration. The findings of our previous clinical study suggest that pelvic incidence–lumbar lordosis mismatch, i.e., ΔPILL $\geq 15°$, could potentially predispose patients to ASD, possibly due to adverse segmental joint loading conditions in the adjacent segments. Furthermore, following fusion of lumbar spine segments, joint loads in the adjacent segments may be even more adverse in patients with a predisposing spino-pelvic alignment. Therefore, it was hypothesized that type A and B alignments result in different segmental joint loads in the prospective epifusional adjacent motion segment. As measuring in vivo joint loads is not readily possible from an ethical and technical point of view, musculoskeletal modeling and simulation provide a valuable tool to investigate joint reaction forces [8–10]. A patient-specific modeling study based on the preoperative radiographs was, therefore, carried out to compute intervertebral joint loads. The models were created such that spino-pelvic anatomy was matched to the radiographs, whereas body mass and height were normalized to obtain comparative results. Subsequently, results from subjects with ASD and with type B alignment were compared to those from controls (CTRL) and with type A alignment, respectively.

Methods

Preoperative radiographs of all 84 patients from our previous study were considered for inclusion. Three patients were excluded due to insufficient radiograph quality to allow proper landmark identification. Landmarks for the locations and orientations of vertebrae T12 to L5, sacrum and center of the hip joints were identified on X-rays (Fig. 1) of the remaining 81 patients. Reference points for the positioning of the bones represented by rigid body bone geometries were then automatically derived from these landmarks and spino-pelvic alignment was characterized by calculation of LL, PI, sacral slope and pelvic tilt. Differences between PI and LL were computed, and for the grouping of patients a ΔPILL threshold of 15° was adopted on the basis of a preceding retrospective clinical study (accompanying ESJ manuscript, in revision).

Modeling and model validation

A musculoskeletal model for the lumbar spine available on simtk.org [9] comprising 210 muscle fascicles was adopted and revised for being automatically adjusted according to the landmarks denoting an individual sagittal spino-pelvic

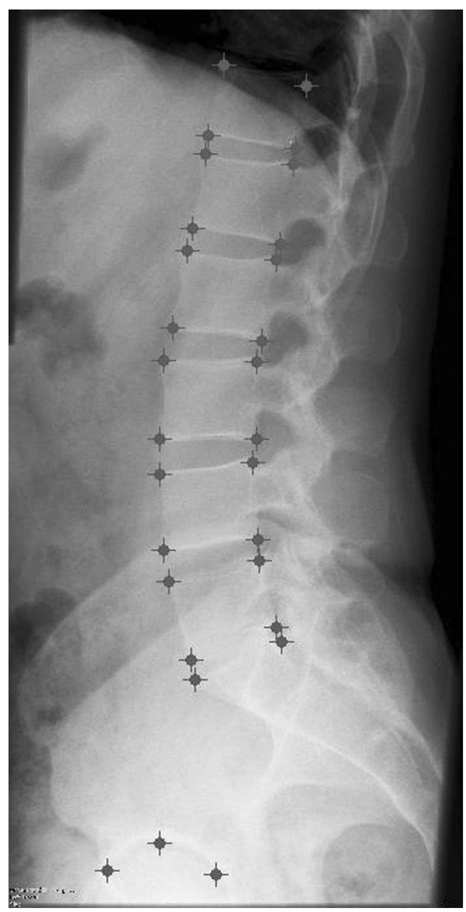

Fig. 1 X-ray with selected landmarks for the characterization of sagittal alignment. These points are later transferred by a custom written MATLAB script into an alignment-specific model in the musculoskeletal simulation software

configuration. A constant scaling factor was employed for all bones. Readjustments of segmental centers of mass ensured average locations according to Pearsall et al. [11]. Additional model modifications were carried out to facilitate relocation and reorientation of bones when the base model is adapted to patient-specific anatomical configurations. Vertebrae local coordinate systems were placed on the midpoint of the posterior vertebral edge and the axes aligned as shown in Fig. 2. Besides advantages during model adaptation, these reference systems allow a simple yet effective interpretation of intervertebral joint load results.

Model validation was performed by comparing relative change of compressive forces between upright and flexed postures to intradiscal pressure (IDP) [12, 13] normalized to upright standing. Shear forces were compared to those from other published muscle-driven numerical models [14–16]. Finally, a qualitative assessment of total forces was performed by comparing in vivo VBR forces [17] over the course of a flexion motion from 0° to 30°.

Generation and analysis of patient-specific models

The validated model served as a base from which all patient-specific models were derived by adjustments of spino-pelvic configuration and scaling of muscle properties to altered lengths.

While the supero-inferior dimension of the base model was kept constant, all other dimensions were scaled accordingly to maintain the relative anatomic positioning. Pelvic orientation (though not necessarily pelvic tilt) was assumed to be neutral in all subjects, as radiographs were all taken in standing posture. The process from reading landmarks to the generation of the models was supported by a semi-automatic MATLAB routine (MATLAB R2012a, TheMathWorks Inc., USA) custom written by MS.

Simulations were performed using custom written MATLAB scripts to run a batch analysis in OpenSim. Further details on procedure and analysis can be found in the OpenSim publication by Delp et al. [18]. Results included muscle activation, muscle forces and joint reactions for all muscles and joints present in the model. In the present study, however, only IVD loads are discussed, distinguishing between shear and compression components according to the coordinate systems described above. The simulated motion represents uniform forward/backward bending at a speed of ~23°/sec which is within the normal range for activities of daily living [19, 20]. Investigated motion has been limited to the range from upright standing to 30° forward inclination, representing limits that can be reached by most people between 51 and 75 years old according to Consmüller et al. [21]. The segmental motion constraints for the non-fused case were adopted from Christophy et al. [9] and for the post-fusion state from Akamaru et al. [4] (L4–L5 fusion) and Auerbach et al. [3] (L4–S1 fusion). Kinematic constraints for all cases are summarized in Table 1.

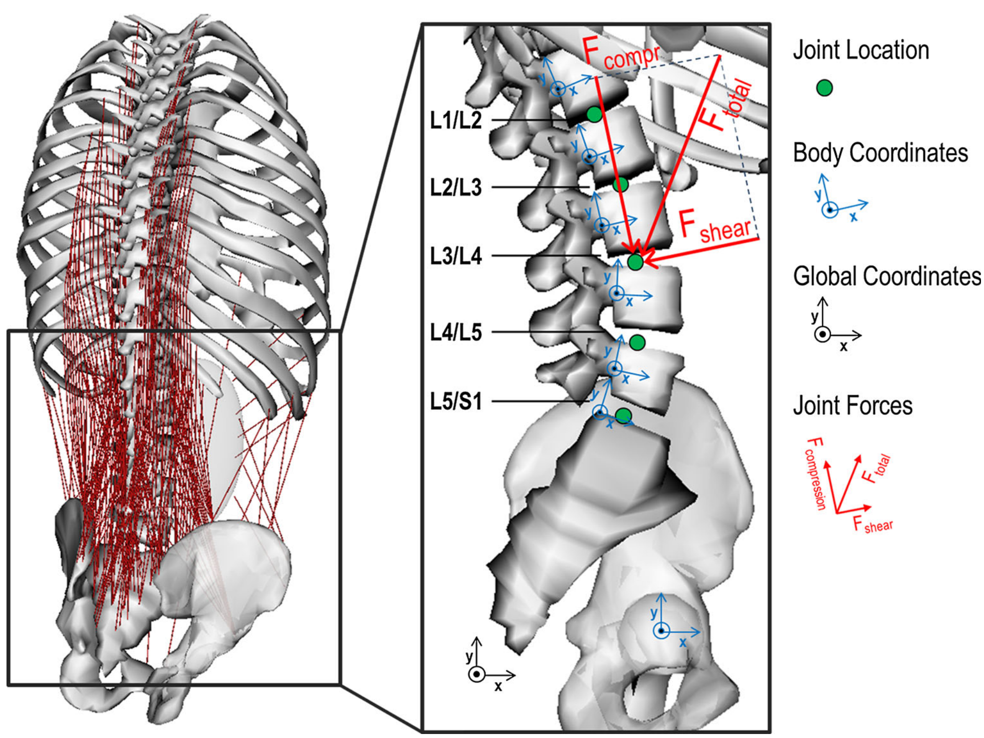

Fig. 2 The musculoskeletal model of the trunk with a detailed representation of the lumbar spine. The newly located and oriented body-specific coordinate systems are shown in *blue*; locations of lumbar ball and socket joints are indicated by *green dots*. Calculated forces are joint reactions acting on the parent body of the considered joint, and are also reported in this body's coordinate system. Accordingly, a positive *x*-component means anterior shear and a positive *y*-component axial compression, as shown by *red arrows* for the L3–L4 intervertebral joint

Table 1 Segmental motion constraints for the unfused state and simulated fusions L4–L5 and L4–S1 according to Akamaru et al. [4] and Auerbach et al. [3], respectively

	L1	L2	L3	L4	L5
No fusion	0.255	0.231	0.204	0.185	0.125
L4–L5 fusion	0.255	0.231	0.286	0.043	0.186
L4–S1 fusion	0.255	0.231	0.472	0.021	0.021

Numbers describe the fraction of lumbar flexion that is covered by vertebrae L1–L5. Sacrum's position remains unchanged, and the thoracic spine is modeled rigidly so that it does not contribute to overall flexion angle (rigid)

Statistics

Data on intervertebral joint loads were not normally distributed and, therefore, analyzed using a Wilcoxon signed rank test for paired (i.e., before/after fusion values) and Mann–Whitney *U* test for unpaired testing (i.e., type A vs. type B alignment). A confidence interval of 0.95 was chosen as the criteria for significance. All analysis was performed in MATLAB using the statistics toolbox (MATLAB R2012a, TheMathWorks Inc., USA).

Results

Model validation

Simulations with the base model showed that compression forces increased similarly as measured by VBR [17] for the corresponding level L1–L2 (Fig. 3a); At level L4–L5 and for a posture of 30° flexion, the model reached 239 % of its initial value in upright standing, while in vivo IDP assessments in the L4–L5 IVD from Wilke et al. [13] on a healthy subject (70 kg, 168 cm) and Sato et al. [12] on 8 subjects (mean 73 kg, 173 cm) evidenced 220 and 250 %, respectively.

Shear force predicted by the OpenSim base model at level L4–L5 in upright posture was 25 N, which lies well within the range of −15 to 90 N reported by several other modeling studies [14–16]. However, differences between model prediction and VBR measurements [17] existed: Shear load at level L1–L2 in upright posture was predicted by the model to be −100 N, while the VBR measured 24 N in vivo. In 30° forward flexed position, the model-based value was close to 0 N as opposed to the VBR load which has increased to 120 N. Although absolute differences are remarkable, the change of shear when moving from an upright standing to a flexed posture was in the same range (Fig. 3b).

Comparing the normalized resultant total force between the model and the VBR revealed a similar trend and an overall increase of about 100 % between upright and 30° flexed posture (Fig. 3c).

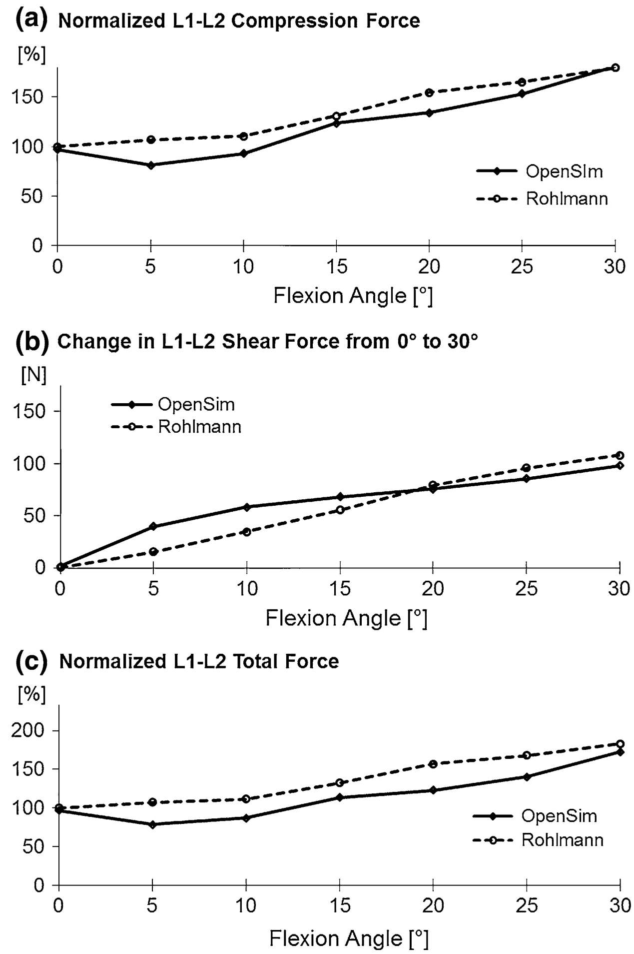

Fig. 3 Model validation: simulations with the base model showed that L1–L2 joint forces increased similarly as in vivo forces measured by a VBR replacing vertebrae L1 [17] for compression normalized to upright standing (**a**), absolute shear (**b**), and normalized resultant total force (**c**)

Effect of alignment on segmental joint reaction forces

Compression and shear forces were plotted against the alignment parameter ΔPILL and a linear best-fit line was determined. A correlation between the parameters could be identified in both upright standing and 30° forward flexed posture using Pearson's correlation. Compression forces exhibited significant correlations with ΔPILL in the upright standing and 30° forward flexed position ($r = -0.29$, $p = 0.008$ and $r = 0.40$, $p < 0.001$, respectively) (Fig. 4a). Significant correlations were likewise found for shear forces (upright standing: $r = 0.36$, $p < 0.001$; 30° forward flexion: $r = 0.48$, $p < 0.001$) (Fig. 4b). Although results suggest interdependence between ΔPILL and IVD loads, the correlations were of moderate magnitude, indicating that not all variability in joint reaction forces can be explained by the parameter ΔPILL. Nonetheless, ΔPILL was significantly correlated with shear and compression forces in 30° forward flexion, in contrast to the lack of correlation using linear regressions based on PI as a predictor variable. In the upright position on the other hand, correlations between joint reaction forces and both anatomical measures (ΔPILL and PI) were similarly strong and significant. Interestingly, analyzing correlations groupwise revealed that joint loads in subjects with alignment of Type B never exhibited significant correlations with either ΔPILL or PI, whereas joint loads in Type A subjects were correlated significantly with ΔPILL in all evaluated cases, except for compression in upright standing.

Patient-specific analysis of 0°–30° forward flexion prior to fusion and comparison of the ASD and CTRL groups revealed the following characteristic differences in force change over the specified range of motion (Fig. 5a; Table 2): at the prospective upper adjacent segment (L3–L4), compression loads were higher but not significant in the ASD group with a 4 % increase ($p = 0.219$) while shear loads were significantly higher in the ASD group by 30 % ($p = 0.023$). At the prospective fusion level (L4–L5), yet still in its state prior to fusion, compression forces were only marginally higher in the ASD group with a non-significant difference of approximately 3 % ($p = 0.445$). Computed shear load changes on the other hand proved to be 41 % larger in the ASD group when compared to the CTRL group ($p = 0.005$).

The same simulation data were subsequently grouped according to alignment classified by ΔPILL into type A and B and again the increase in compression and shear forces from upright to 30° flexed posture was compared between both groups (Fig. 5b; Table 2). In contrast to the previous grouping, compression force changes at level L3–L4 were now significantly higher in type B alignments by a relative difference of 8 % ($p = 0.041$). Shear forces were 32 % higher in the group with type B alignment ($p = 0.015$). At level L4–L5, compression loads were significantly higher by 9 % in type B alignments ($p = 0.003$), while the difference in shear loads was less pronounced (14 %) and not significant ($p = 0.099$).

Overall, the simulations using patient-specific models in the unfused spine indicate that there was a relationship

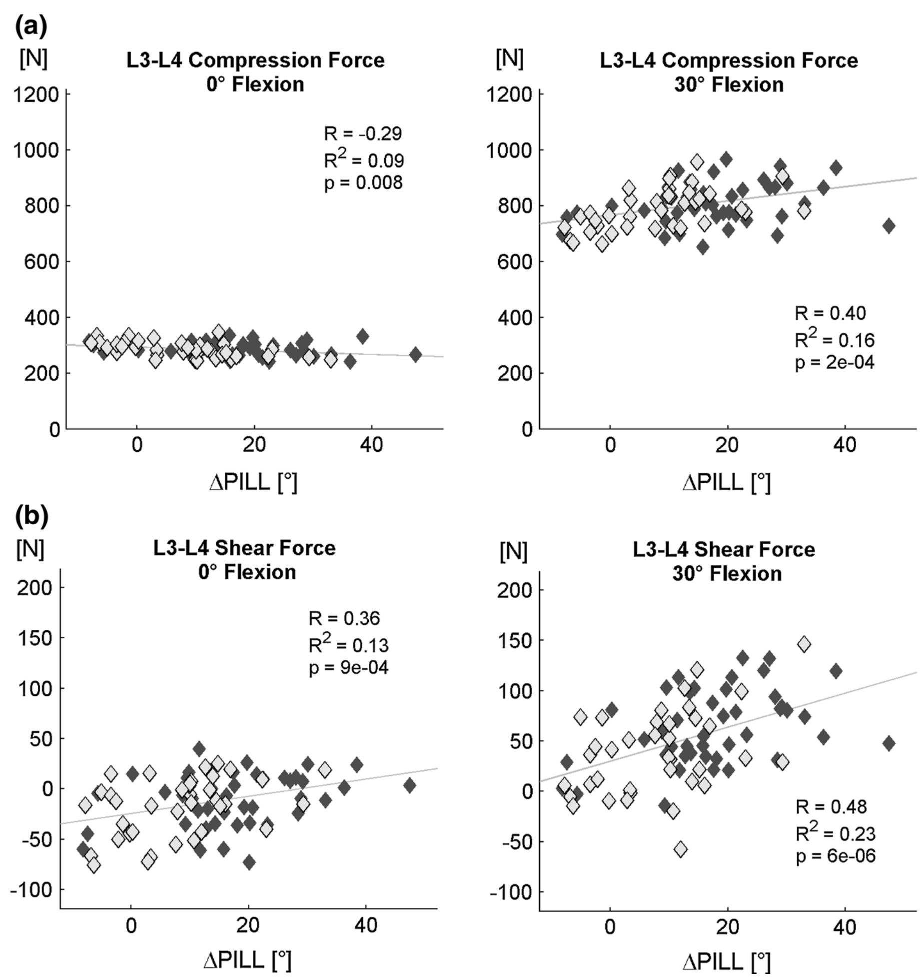

Fig. 4 Compression (**a**) and shear forces (**b**) in the prospective adjacent segment L3–L4 in the unfused spine are correlated with spino-pelvic alignment according to the parameter ΔPILL in 0° and 30° flexion. With increasing ΔPILL compression as well as shear forces increase in the prospective adjacent segment ($p < 0.01$ for all correlations, Pearson's correlation coefficients for compression $r = -0.29$ and $r = 0.40$ and for shear $r = 0.36$ and $r = 0.48$ for 0° and 30° flexion respectively; ASD subjects *black*, CTRL subjects *white*)

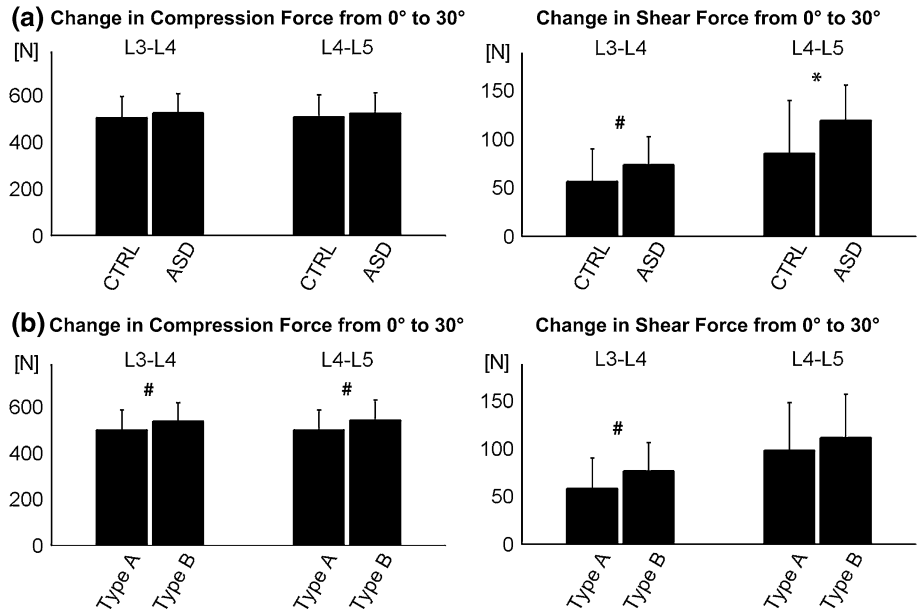

Fig. 5 **a** Changes in shear and compression forces in the unfused spine at L3–L4 and L4–L5 from 0° to 30° flexion comparing the ASD to the CTRL group. It appears that simulations in spines which clinically presented with adjacent segment disease showed significantly greater shear forces in both levels, whereas the differences for compression were not significant for compression. In **b,** the same is shown for simulations comparing a type A (ΔPILL <15°) to a type B alignment (ΔPILL ≥15°). Significantly increased shear forces could be seen at L3–L4 and L4–L5 in type B alignments compared to type A. Compression forces did not differ significantly (levels of significance: $*p \leq 0.01$; $\#p \leq 0.05$)

Table 2 Prior to fusion: increase in joint reaction force from upright standing position 0° to 30° flexion at the prospective adjacent level L3–L4 and the fusion level L4–L5

	IVD L3–L4 (prospective adjacent level)		IVD L4–L5 (prospective fusion level)	
	Compression (*N*)	Shear (*N*)	Compression (*N*)	Shear (*N*)
CTRL	+503.0 (91.0)	+56.2 (33.5)†	+507.0 (93.6)	+85.3 (54.3)†
ASD	+525.4 (80.4)	+73.3 (29.1)†	+523.4 (86.1)	+119.9 (36.7)†
Type A	+499.7 (87.3)†	+58.2 (31.8)†	+499.2 (87.5)†	+98.3 (49.8)
Type B	+538.9 (78.5)†	+76.6 (29.8)†	+542.4 (87.2)†	+111.6 (45.5)

Standard deviations within the groups are given in parentheses. The data are grouped according the development of adjacent segment degeneration with need for revision surgery (CTRL and ASD) or the classification of alignment based on ΔPILL (type A and B)

† Significant differences between the groups ($p < 0.05$)

between spino-pelvic alignment and segmental joint reaction forces and that disparities in alignment as described as the difference between PI and LL (ΔPILL) largely led to an increase in segmental shear forces and to a lesser extent compression forces in the prospective adjacent segments of L4–L5 single level and L4–S1 bisegmental fusions.

Effect of fusion on joint reaction forces in the adjacent segment

The effect of fusion on the loads in the adjacent level IVD was investigated separately for groups with type B and A alignment. Both L4–L5 and L4–S1 fusions were simulated and absolute forces at the adjacent level L3–L4 in upright standing position were compared between pre- and post-fusion state (Tables 3, 4). Moreover, the effect of fusion on force changes during movement from 0° upright standing to 30° forward flexed posture was analyzed (Fig. 6).

In upright standing, no significant alterations in absolute loads due to single-level L4–L5 fusion were observed between type B and A alignment. Changes in compression forces were <1 % on average and magnitudes of shear loads were marginally lowered by L4–L5 fusion in both groups (−0.8 N in both groups, or −11 % for type B and −4 % for type A). Effects of L4–S1 bisegmental fusion were in a similar range though significantly different between type A and B alignment (shear forces: −1.0 N in type B (−14 %) and +0.4 N (+2 %) in type A; compression forces: +0.2 N in type B (+0 %) and +8.1 N in type A (+3 %)).

In contrast to these small absolute changes in force that characterized the fused spine in an upright standing position, forward bending after simulated fusion caused consistently higher shear forces in 30° forward flexed position than prior to fusion and a significantly larger increase was

Table 3 Absolute shear forces in two positions (upright standing and 30° flexion) at the adjacent level to fusion (L3–L4) prior to fusion and after L4–L5 and L4–S1 arthrodesis

Shear adjacent level L3–L4		Shear (*N*) pre-fusion	Shear (*N*) L4–L5 fusion	Shear (*N*) L4–S1 fusion
0° upright	Type A	−17.4 (29.0)	−16.6 (28.7)$^{\Delta}$	−17.8 (30.2)
	Type B	−7.1 (24.7)	−6.3 (24.8)$^{\Delta}$	−6.1 (26.6)
30° flexion	Type A	40.9 (40.0)†	49.9 (41.5)$^{\dagger,\Delta}$	91.4 (41.4)$^{\dagger,\Delta}$
	Type B	69.5 (37.9)†	80.5 (38.7)$^{\dagger,\Delta}$	129.3 (38.1)$^{\dagger,\Delta}$

For each group, standard deviations are given in brackets

† Significant differences between groups of type A and B alignment

$^{\Delta}$ significant differences between pre- and post-fusion states ($p < 0.05$)

Table 4 Absolute compression forces in two positions (upright standing and 30° flexion) at the adjacent level to fusion (L3–L4) prior to fusion and after L4–L5 and L4–S1 arthrodesis

Compression adjacent level L3–L4		Compression (*N*) pre-fusion	Compression (*N*) L4–L5 Fusion	Compression (*N*) L4–S1 Fusion
0° upright	Type A	288.5 (24.6)†	286.6 (24.9)	296.6 (23.1)$^{\Delta}$
	Type B	277.6 (26.6)†	278.6 (26.5)	277.8 (23.3)
30° flexion	Type A	788.1 (72.0)	793.9 (71.6)$^{\Delta}$	736.8 (61.8)$^{\dagger,\Delta}$
	Type B	816.5 (75.9)	826.3 (74.8)$^{\Delta}$	777.4 (65.8)$^{\dagger,\Delta}$

For each group, standard deviations are given in brackets

† Significant differences between groups of type A and B alignment

$^{\Delta}$ Significant differences between pre- and post-fusion states ($p < 0.05$)

observed in subjects with type B alignment. Specifically, changes due to L4–L5 fusion were +11.0 N in type B and +9.0 N in type A, with even higher changes in shear forces after L4–S1 fusion of +59.8 N in type B and +50.5 N in type A subjects. Relatively, at 30° forward flexion, lumbar fusion caused an approximately 20 % higher increase in shear forces in a type B compared to type A alignment. On the other hand, compressive forces were affected to similar extents in type A and B alignment by both types of fusion. L4–L5 fusion tended to increase compressive forces in the adjacent IVD, while L4–S1 fusion diminished or maintained compressive loads (Fig. 6a). Although some discrepancy in mean values between type A and B alignment was apparent, statistical dispersion was such that significance was not achieved.

In summary, force analysis during a forward bending motion from upright standing to 30° flexion compared between pre- and post-fusion states for subjects of type A and B alignment (Tables 2, 3, 4; Fig. 6) indicated that shear force changes after fusion were increased for both types of evaluated fusion with significantly larger changes in type B subjects. Significant differences were furthermore consistently found in compression forces, yet L4–S1 fusion led to a generally reduced range of compression loads while L4–L5 seemed to enlarge it.

Discussion

While the importance of spinal balance and spino-pelvic alignment has been widely reported [6, 7, 22, 23] and biomechanical consequences on the motion segments seem evident, the relationship between PILL mismatch and lumbar segmental joint loads has not been studied in detail. In the present study, alignments were modeled in a patient-specific manner to study segmental joint reaction forces based on the observation from our clinical study that patients with a higher difference between pelvic incidence and lumbar lordosis (ΔPILL) seem to have a higher risk for adjacent segment disease. The results of the simulations indicate that in the unfused spine, spino-pelvic alignment as quantified by the parameter ΔPILL correlates with an increase in shear as well as compression forces in the L3–L4 and L4–L5 motion segments.

Comparing the patient-specific modeling data for the ASD and CTRL groups identified in the previous clinical study reveals a significantly higher change in shear force during movement from upright standing to 30° flexion in the ASD group compared to the CTRL group, whereas for compression forces no significant difference was observed. Grouping the same data according to ΔPILL into type A and B alignment demonstrates even stronger differences in transitional shear force change as well as a significantly higher increase in compression forces in the type B group compared to type A alignment. The differences due to grouping are explained by the fact that type A subjects with ASD and type B subjects without ASD equalize disparities in loads between ASD and CTRL groups to some extent. In contrast, classification according to alignment clearly separates subjects with balanced PI and LL from those who do not seem to compensate for a high PI and consequently fall outside the normal range that has been observed by Vaz et al. [23]. Hence variability between type A and B groups is more pronounced and significant even for the case of compression forces.

Implementing L4–L5 and L4–S1 fusion by changing segmental motion constraints caused an increase of shear forces at intervertebral level L3–L4 in forward flexed postures in type A and B alignments. Slightly higher yet significant differences were observed for type B alignment in the adjacent segment after L4–L5 fusion. Similarly, a higher increase was found in type B after L4–S1 fusion. Fusion-induced changes in compression forces were found for L4–L5 or L4–S1 fusion, and different effects depending on the type of fusion were observed. Increasing muscle forces during forward flexion after single-level L4–L5

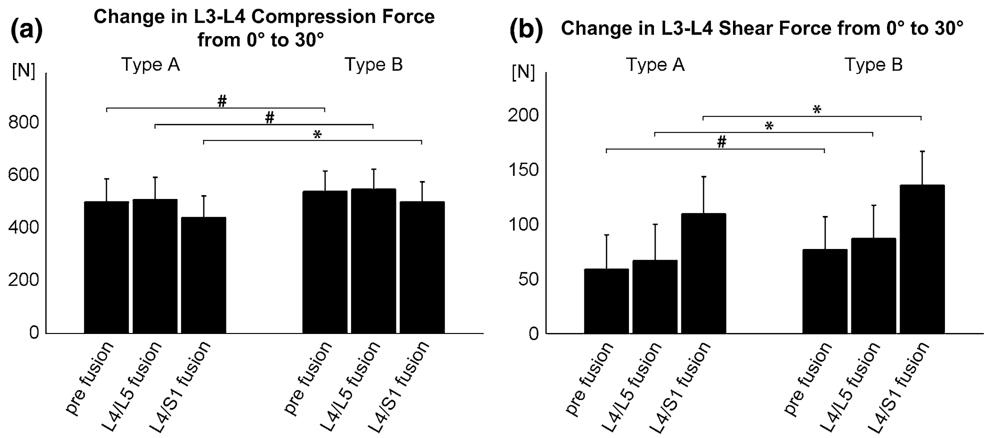

Fig. 6 Intervertebral shear (**a**) and compressive (**b**) loads at the adjacent level L3–L4 after L4–L5 and L4–S1 fusion and for the state prior to fusion. Results are given for alignment type A and B separately (*left* and *right* sets of columns, respectively). Differences between corresponding loads from type A and B alignment were statistically analyzed and levels of significance are indicted by *horizontal bars* using the symbols * for $p \leq 0.01$ and # for $p \leq 0.05$

fusion lead to an increased compressive component, while L4–S1 fusion diminishes compressive loads in favor of shear, because in this case muscle lines of action cannot follow the trunk during forward flexion, thereby changing the relation of muscle force- to disc space-orientation. Furthermore, the characteristically higher joint forces observed in type B alignment in a forward bending posture can be attributed to the tendency for increased recruitment of extensor muscles in this group. This, in turn, likely affects spinal stability but also promotes the risk for injury [24], with potential implications for the development of disc degeneration [25].

As with any modeling study, the data presented are based on assumptions regarding model simplifications, which ultimately may affect the accuracy of results. Limitations of the present model include the lack of intervertebral stiffness, ligaments and intra-abdominal pressure. However, the validation we provide was according to recommended standards [26] and indicates good agreement of predicted joints loads with available data in the literature. Neglecting facet joints is justified since simulations focused on forward bending movements only. As an isolated perspective on the effect of alignment on joint loads was vital, patient-specific factors that were not directly related to spino-pelvic sagittal alignment were kept constant across the simulated population. The sagittal plane anatomy of the lower trunk, however, was reproduced on the basis of each subject's individual X-ray. Regarding model kinematics, no clear relation between anatomy and segmental motion could be elaborated so far, thus the spinal rhythms were employed throughout the whole population. Importantly, despite above-mentioned simplifications, distinctive muscle recruitment patterns and joint reactions resulted for all subjects. Therefore, in every case of the above simplifications, we do not expect any systematic bias to be present between the compared populations and the observed joint loading differences between populations can be confidently tied to differences in spino-pelvic sagittal alignment as expressed by PILL mismatch. Caution must be employed when considering the findings in the context of clinical implications. It should also be noted that joint level biomechanics are likely to play only a partial role in intervertebral disc pathology [25], and that multifactorial consideration of patient-specific factors was not considered in the present study. Such investigations including causative factors beyond sagittal alignment are important grounds for future work.

All computed loads are acting at the joint center and are expressed in the coordinate system superior to the joint (Fig. 2). Given the small average vertebral wedge angles reported by Damasceno et al. [27], the slight mismatch between orientation of endplate and coordinate system is negligible and shear forces can be considered acting along the superior IVD endplate.

The findings of our simulations suggest that shear forces differ to a larger degree than compression forces in different alignments and after fusion. Shear forces acting on the intervertebral joint, therefore, potentially play a significant role in degeneration of the intervertebral disc and subsequently of the motion segment. Shear has been identified as an important loading mode acting on the intervertebral disc, especially in bending and torsion loading [28, 29]. A recent study investigated shear in vivo in a rat model and found that application of a sustained shear force induced degeneration in the intervertebral discs subject to loading as well as in the adjacent segment [30]. The authors particularly found that much lower shear stress is required to induce degenerative changes compared to reported compression stress in similar studies investigating compression forces, concluding that shear may be more detrimental to the intervertebral disc than compressive load. Considering the natural function of the nucleus pulposus and annulus, the disc seems be able to resist compressive forces better than shear forces. It remains to be investigated using finite element models; however, how the cell's perceived mechanical environment depends on the joint reaction forces. While the resulting joint reaction forces reported here cannot be translated directly into micromechanical stimuli at the tissue level, these findings will serve to determine the boundary conditions for such models and will help to deepen the understanding of the effect of segmental joint mechanics on the intervertebral disc in relation to spinal alignment.

In conclusion, patients with a type B alignment and higher PILL mismatch exhibit higher shear stresses before and after fusion, which may account for the clinical observation that patients with a type B alignment seem to be predisposed to adjacent segment degeneration after lumbar fusion, suggesting that the increased shear may be responsible for accelerated degeneration in these cases. Although fusion increases shear and to some extent compression forces further, patients with a type B alignment exhibit higher shear stresses at their intervertebral joints already prior to fusion compared to type A alignment, potentially indicating an unfavorable natural history. By providing a biomechanical explanation for the observations in the previous clinical study, this study gives evidence for the importance of spino-pelvic alignment and, therefore, matching pelvic incidence and lumbar lordosis for the outcome of lumbar fusion.

Conflict of interest None.

References

1. Xia X-P, Chen H-L, Cheng H-B (2013) Prevalence of adjacent segment degeneration after spine surgery: a systematic review and meta-analysis. Spine 38:597–608
2. Zhu Q, Itshayek E, Jones CF, Schwab T, Larson CR, Lenke LG, Cripton PA (2012) Kinematic evaluation of one- and two-level Maverick lumbar total disc replacement caudal to a long thoracolumbar spinal fusion. Eur Spine J 21(Suppl 5):S599–S611
3. Auerbach JD, Wills BPD, McIntosh TC, Balderston RA (2007) Evaluation of spinal kinematics following lumbar total disc replacement and circumferential fusion using in vivo fluoroscopy. Spine 32:527–536
4. Akamaru T, Kawahara N, Tim Yoon S, Minamide A, Su Kim K, Tomita K, Hutton WC (2003) Adjacent segment motion after a simulated lumbar fusion in different sagittal alignments: a biomechanical analysis. Spine 28:1560–1566
5. Schmidt H, Galbusera F, Rohlmann A, Zander T, Wilke H-J (2012) Effect of multilevel lumbar disc arthroplasty on spine kinematics and facet joint loads in flexion and extension: a finite element analysis. Eur Spine J 21(Suppl 5):S663–S674
6. Pellet N, Aunoble S, Meyrat R, Rigal J, Le Huec JC (2011) Sagittal balance parameters influence indications for lumbar disc arthroplasty or ALIF. Eur Spine J 20(Suppl 5):647–662
7. Barrey C, Roussouly P, Perrin G, Le Huec J-C (2011) Sagittal balance disorders in severe degenerative spine. Can we identify the compensatory mechanisms? Eur spine J 20(Suppl 5): 626–633
8. Galbusera F, Wilke H-J, Brayda-Bruno M, Costa F, Fornari M (2013) Influence of sagittal balance on spinal lumbar loads: a numerical approach. Clin Biomech 28(4):370–377. doi:10.1016/j.clinbiomech.2013.02.006
9. Christophy M, Faruk Senan NA, Lotz JC, O'Reilly OM (2012) A musculoskeletal model for the lumbar spine. Biomech Model Mechanobiol 11:19–34
10. De Zee M, Hansen L, Wong C, Rasmussen J, Simonsen EB (2007) A generic detailed rigid-body lumbar spine model. J Biomech 40:1219–1227
11. Pearsall DJ, Reid JG, Livingston LA (1996) Segmental inertial parameters of the human trunk as determined from computed tomography. Ann Biomed Eng 24:198–210
12. Sato K, Kikuchi S, Yonezawa T (1999) In vivo intradiscal pressure measurement in healthy individuals and in patients with ongoing back problems. Spine 24:2468–2474
13. Wilke H-J, Neef P, Hinz B, Seidel H, Claes L (2001) Intradiscal pressure together with anthropometric data–a data set for the validation of models. Clin Biomech 16(Suppl 1):S111–S126
14. Kim K, Kim YH (2008) Role of trunk muscles in generating follower load in the lumbar spine of neutral standing posture. J Biomech Eng 130:041005
15. Arjmand N, Gagnon D, Plamondon A, Shirazi-Adl A, Larivière C (2009) Comparison of trunk muscle forces and spinal loads estimated by two biomechanical models. Clin Biomech 24:533–541
16. El-Rich M, Shirazi-Adl A, Arjmand N (2004) Muscle activity, internal loads, and stability of the human spine in standing postures: combined model and in vivo studies. Spine 29:2633–2642
17. Rohlmann A, Graichen F, Kayser R, Bender A, Bergmann G (2008) Loads on a telemeterized vertebral body replacement measured in two patients. Spine 33:1170–1179
18. Delp SL, Anderson FC, Arnold AS, Loan P, Habib A, John CT, Guendelman E, Thelen DG (2007) OpenSim: open-source software to create and analyze dynamic simulations of movement. IEEE Trans Biomed Eng 54:1940–1950
19. Ikeda E, Schenkman M, Riley P, Hodge W (1991) Influence of age on dynamics of rising from a chair. Phys Ther 71:473–481
20. Krebs DE, Wong D, Jevsevar D, Riley PO, Hodge WA (1992) Trunk kinematics during locomotor activities. Phys Ther 72:505–514
21. Consmüller T, Rohlmann A, Weinland D, Druschel C, Duda GN, Taylor WR (2012) Velocity of lordosis angle during spinal flexion and extension. PLoS ONE 7:1–7
22. Mehta VA, Amin A, Omeis I, Gokaslan ZL, Gottfried ON (2012) Implications of spinopelvic alignment for the spine surgeon. Neurosurgery 70(3):707–721. doi:10.1227/NEU.0b013e31823262ea
23. Vaz G, Roussouly P, Berthonnaud E, Dimnet J (2002) Sagittal morphology and equilibrium of pelvis and spine. Eur Spine J 11:80–87
24. Granata KP, Wilson SE (2001) Trunk posture and spinal stability. Clin Biomech (Bristol, Avon) 16:650–659
25. Hadjipavlou AG, Tzermiadianos MN, Bogduk N, Zindrick MR (2008) The pathophysiology of disc degeneration: a critical review. J Bone Joint Surg Br 90:1261–1270
26. Lund ME, de Zee M, Andersen MS, Rasmussen J (2012) On validation of multibody musculoskeletal models. Proc Inst Mech Eng Part H J Eng Med 226:82–94
27. Damasceno LHF, Catarin SRG, Campos AD, Defino HLA (2006) Lumbar lordosis: a study of angle values and of vertebral bodies and intervertebral discs role. Acta Ortop Bras 14:193–198

28. Adams MA, Hutton WC (1981) The relevance of torsion to the mechanical derangement of the lumbar spine. Spine 6:241–248
29. Barbir A, Godburn K, Michalek A, Lai A (2011) Effects of torsion on intervertebral disc gene expression and biomechanics, using a rat tail model. Spine 36:607–614
30. Kim J, Yang SJ, Kim H, Kim Y, Park JB, Dubose C, Lim TH (2012) Effect of shear force on intervertebral disc (IVD) degeneration: an in vivo rat study. Ann Biomed Eng 40(9):1996–2004. doi:10.1007/s10439-012-0570-z